Superfluidity of ^{4}He Confined in Microscopic Bubbles in Copper

E. G. Syskakis and F. Pobell
Institut für Festkörperforschung, Kernforschungsanlage Jülich, D-5170 Jülich, West Germany, and Physikalische Institut, Universität Bayreuth, D-8580 Bayreuth, West Germany[a]
and
H. Ullmaier
Institut für Festkörperforschung, Kernforschungsanlage Jülich, D-5170 Jülich, West Germany
(Received 30 August 1985)

We have created extremely small and independent Bose systems by confining ^{4}He in bubbles of radius of less than 110 Å in Cu foils. The size distribution and density of the bubbles were adjusted by annealing the samples and were determined by transmission electron microscopy. At low temperatures the confined helium becomes first solid, then liquid, and eventually superfluid as the mean bubble size is increased by annealing. The modification of superfluidity in this new confining geometry by size effects has been investigated by low-temperature calorimetry.

PACS numbers: 64.70.Dv, 65.20.+w, 67.40.Kh, 67.70.+n

Because of its purity and homogeneity, liquid helium is a unique system for studies of finite-size effects. The superfluid transition of helium has been investigation in various confining geometries, e.g., helium films on planar substrates, and helium in Vycor glass, Nuclepore filters, or fine powders. Observed modifications of superfluidity were in qualitative agreement with expectations of the mean-field theory and were also compared to finite-size scaling arguments. Experimental data could not, however, always be used to test theoretical predictions because of insufficient knowledge and of complexity of the confining system. In the case of porous materials an additional disadvantage is the connectivity of the pores, which may reduce the effectiveness of the confinement.

Following a different approach we have confined high-pressure helium gas in nonconnected cavities (bubbles) in Cu. At low temperatures the confined helium liquifies. Here we report our results on low-temperature calorimetry, particularly the effects of pore size on the superfluid transition in bubbles of average radius between 25 and 108 Å. Low-temperature calorimetric evidence for superfluidity of helium in voids in irradiated solids has previously been reported by Keesom and co-workers,[1] Aslanian and Weil,[2] and Gmelin[2]; indications for size effects can be inferred from the data in Ref. 2.

This new confining geometry is well defined and is topologically simple as we show by transmission electron microscopy (TEM). It creates an ensemble of extremely small Bose systems completely isolated from each other and consisting of about 10^4 helium atoms each. Our work presents, in addition, experimental thermodynamic support for the properties of helium in small bubbles in a metal.

Helium is practically insoluble in metals.[3] Therefore, when helium is injected or produced in a metal it precipitates into microscopic bubbles whose size can be increased by annealing of the specimens. Significant reemission of helium from bulk metallic specimens charged with low helium concentrations is observed only in the neighborhood of the melting temperature of the metal. The gas pressure in the bubbles is in the kilobar range so that its density can be very high.[4-6] According to the equation of state,[7] *liquid* helium is expected to exist in Cu in bubbles of radius $r \gtrsim 40$ Å at low temperatures.

We have introduced helium into 99.999%-pure Cu disks of 7-mm diam × 100-μm thickness by implanting them with α particles at room temperature.[8] A homogeneous deposition of α particles has been achieved by use of an energy degrader to vary the energy of a wobbled cyclotron beam from 28 MeV to zero. The implanted amount of helium has been determined by the outgassing of several pieces of the specimens. Two pairs of specimens have been produced: One pair with 690 at. ppm and the second with 1860 at. ppm He/Cu, resulting in helium masses of 1.19 and 3.20 μg, respectively. One member of each pair has been used for low-temperature calorimetry, while the second was cut into disks of 3-mm diameter and used for TEM investigations.

Heat-capacity measurements were performed between 1.5 and 7 K in a calorimeter described elsewhere.[8] It was cooled without exchange gas. The specimen holder was a sapphire plate ($12\times8\times0.08$ mm^3) with an evaporated Constantan film as heater and a thin carbon thermometer.

The Cu sample was attached to the sapphire plate by 1 mg of Apiezon N grease. The specimen holder was supported by four Pt-92%–W-8% wires of 25-μm diameter which provided weak thermal contact to a regulated isothermal shield. The heat capacity of helium in the specimen (accuracy of 5% below 2.5 K, 10% at 5

K) was obtained by subtracting from the total heat capacity the addenda and Cu contributions (each about 1 μJ/K at 2.2 K).

Heat-capacity measurements directly after the implantation and again after annealing of the 690-at.-ppm specimen at $T_a = 830$ K for $t_a = 2$ h showed no contribution of helium to within $\pm 3\%$. These observations indicate that the helium was still a high-density solid in clusters and/or tiny bubbles ($r \sim 10$ Å) with at most a very small contribution to the heat capacity at low temperatures, as also observed in Refs. 1 and 2.

Figure 1 shows the heat capacity of helium after repeated annealing of the specimens in a vacuum 5×10^{-7} mbar. Details of the annealing programs are given in Table I. After annealing of the specimen with

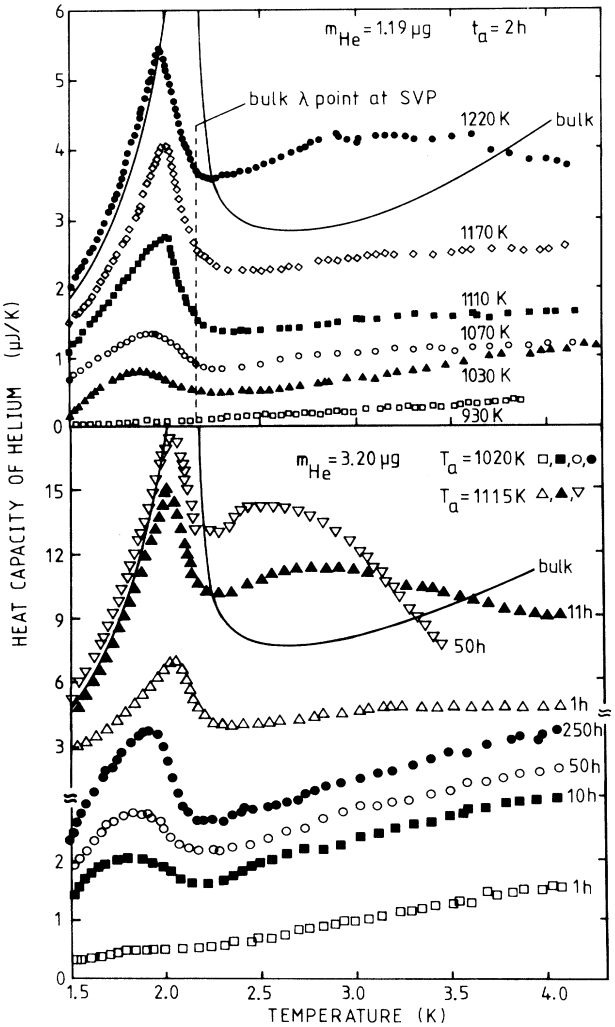

FIG. 1. Heat capacity of helium confined in bubbles in Cu after vacuum annealing of the specimens at the temperatures given in the figure. The continuous lines show the heat capacity of the corresponding mass of bulk liquid helium at saturated vapor pressure (SVP).

690 at. ppm helium at $T_a = 930$ K, the first contribution due to helium was observed. It is in excess of the heat capacity of the corresponding amount of bulk solid helium. The observed enhancement may be attributed to the heat of melting of helium or to some liquid already present in the larger bubbles of the size distribution. Alternatively, it might be due to a 50% decrease of the Debye temperature of solid helium in the 25-Å bubbles.

Upon further annealing we observed a substantial increase in the heat capacity of the helium with increasing T_a, and a growing anomaly at $T \lesssim 2$ K. The latter first appeared as a small bump at $T_p \approx 1.8$ K and then developed progressively to a sharp and growing peak, thus becoming the dominant contribution to the total heat capacity. Simultaneously T_p increased slightly to higher temperatures, reached 1.99 ± 0.02 K (2.05 ± 0.02 K) for the first (second) sample, and then stayed essentially constant in spite of the still growing bubble size (see Table I). We have taken heat-capacity data both during cooling and warming of our specimen into the transition region without detecting any sign of hysteresis. We attribute these heat-capacity peaks to a second-order superfluid transition.

After each annealing step a TEM specimen has been electropolished by a double-jet technique and examined in a TEM.[8] The transparent area was located approximately 50 μm below the original surfaces of the specimen, so that the bubble-size data of Table I should not have been influenced by surface effects. A typical TEM picture of helium bubbles partly located along dislocations of the Cu matrix is shown in Fig. 2. The bubbles are clearly faceted, which confirms that the bubbles were grown in thermal equilibrium.[9] In the following we neglect the faceting and discuss the bubbles as "spheres." Figure 2 demonstrates the homogeneity of the confinement as well as the zero connectivity of the bubbles. Enlarged prints of such micrographs were evaluated with a particle size analyzer, yielding the size distributions of bubbles, their average radius, $\bar{r}$, and the half width, Δr, of the size distributions as presented in Table I.[8] In addition, we determined the volume density of the bubbles and found, for example, a value of 8.4×10^{15} cm^{-3} for the specimen of 690 at. ppm when $T_a = 1030$ K, decreasing to 3.5×10^{14} cm^{-3} when $T_a = 1220$ K. The size increase for the isothermal-annealing experiments followed $\ln\bar{r} = 0.07 \ln t_a$.[8]

The evolution of the bubbles is governed by thermodynamic properties of helium in the metal. The bubbles exchange helium at T_a, increasing their average size and decreasing the pressure in them. In a bubble of radius r at thermal equilibrium the pressure is

$$P(T_a) = 2\gamma/r, \quad (1)$$

where we will assume $\gamma = 1.67$ J/m^2 for the specific

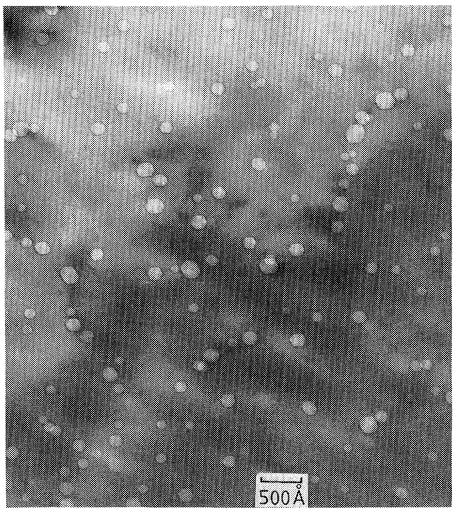

FIG. 2. A typical TEM picture of underfocused helium bubbles in Cu. The bubbles appear as light areas and are clearly faceted.

surface energy of bulk Cu. Combining data of Table I with Eq. (1) and the equation of state for dense helium in bubbles,[7] we calculate the average pressure and density of the helium. According to this calculation, we expect solid helium in bubbles with $r \lesssim 35$ Å. Bubbles with $r = 43$ Å are located at the upper λ point of the phase diagram of bulk helium. This agrees with our observation that we only observed a peak in the heat capacity for $\bar{r} > 37$ Å. The calculation also shows that the liquid-gas equilibrium state is first established in bubbles with $r \approx 60$ Å. Therefore, bubbles with $r > 60$ Å become only partly filled with liquid helium at low temperatures. Assuming for simplicity that the helium then condenses as spherical shells on the inner bubble surface, we can calculate the thickness of these films by assigning a density of 0.147 (0.259) g/cm^3 to the liquid (to a 3.6-Å solid layer at the wall). The film thickness decreases appreciably for increasing r up to $r = 80$ Å, and then approaches the ideal-gas limiting value of about 30 Å estimated at large radii from the relationship $d = 2\gamma m/3k_B T_a \rho$, where m is the mass of the helium atom, k_B is Boltzmann's constant, and ρ is the density of saturated liquid helium.

For the geometry-induced displacement ΔT_λ of the superfluid transition of helium confined in a sphere of radius r, Ginzburg and Sobyanin predict[10]

$$\Delta T_\lambda(r) = (2.53 \times 10^{-11}\ \mathrm{cm}^{3/2}) r^{-3/2}\ \mathrm{K}. \quad (2)$$

For calculation of the expected shifts ΔT_λ we have subtracted from the measured radii a layer of 6 Å of "passivated" solid and normal fluid helium near the bubble wall. The calculated ΔT_λ's are typically a factor of 3 smaller than $T_{\lambda,\mathrm{SVP}} - T_p$. This disagreement indicates that for $\bar{r} < 60$ Å the contribution of the pressure to the displacement of the transition temperature was significant. For $\bar{r} > 60$ Å the discrepancy arises because, as shown above, bubbles are only partly filled with liquid. Consequently, the confining dimension is now the approximately constant thickness of the helium film. This explains why T_p did not increase fur-

TABLE I. Annealing programs and calorimetric and TEM data for the specimen of 690 at. ppm (upper part) and 1860 at. ppm (lower part) helium in Cu. The shifts $\Delta T_\lambda(\bar{r})$ are calculated from Eq. (2) under the assumption of bubbles full of liquid, while those of the last column are calculated by means of our model as explained in the text.

T_a (K)	t_a (h)	$\bar{r}$ (Å)	Δr (Å)	T_p (K)	$T_{\lambda,\mathrm{SVP}} - T_p$ (K)	$\Delta T_\lambda(\bar{r})$ (K)	ΔT_λ (K)
				690 at. ppm He in Cu			
930	2	24.5	16	· · ·	· · ·	0.317	· · ·
1030	2	37.0	23	1.83 ± 0.04	0.34 ± 0.04	0.146	· · ·
1050	2	41.5	17	1.90 ± 0.04	0.27 ± 0.04	0.119	· · ·
1070	2	49.5	25	1.93 ± 0.04	0.24 ± 0.04	0.088	0.30
1090	2	56.0	26	1.99 ± 0.03	0.18 ± 0.03	0.071	0.16
1110	2	58.5	28	2.01 ± 0.02	0.16 ± 0.02	0.066	0.11
1130	2	68.5	33	1.96 ± 0.01	0.21 ± 0.01	0.051	0.10
1170	2	82.5	37	2.00 ± 0.01	0.17 ± 0.01	0.038	0.14
1220	2	108.0	42	1.97 ± 0.01	0.20 ± 0.01	0.024	0.15
				1860 at. ppm He in Cu			
1020	1	35.0	17	· · ·	· · ·	0.162	· · ·
1020	10	41.0	20	1.80 ± 0.04	0.37 ± 0.04	0.145	· · ·
1020	50	46.0	22	1.85 ± 0.04	0.32 ± 0.04	0.100	0.49
1020	250	51.0	25	1.95 ± 0.03	0.22 ± 0.03	0.083	0.30
1115	1	66.0	31	2.05 ± 0.01	0.12 ± 0.01	0.054	0.10
1115	11	76.5	34	2.02 ± 0.01	0.15 ± 0.01	0.042	0.13
1115	50	82.5	37	2.06 ± 0.01	0.11 ± 0.01	0.038	0.14

ther as the bubbles grew above 60 Å. With the calculated film thickness d (corrected for substrate effects) we used Eq. (2) with $r = d$ [10] to estimate $\Delta T_\lambda(d)$ in the bubbles which contained helium films ($\bar{r} > 60$ Å). For the liquid-filled bubbles ($\bar{r} < 60$ Å) we used the calculated average liquid-helium densities to estimate the pressure-induced shift $\Delta T_\lambda(P)$ of the λ point. To that we added $\Delta T_\lambda(\bar{r})$ deduced from Eq. (2) (after subtracting a thickness of 6 Å from $\bar{r}$) assuming that the pressure- and geometry-induced displacements of T_λ are additive. The results of these calculations are shown in the last column of Table I. We consider the agreement with the observed data for $T_p > 1.9$ K as satisfactory in view of the uncertainties involved.

The agreement between measured and calculated shifts is no longer fulfilled for samples with $\bar{r} < 45$ Å and $T_p < 1.9$ K. Assuming the pressure- and geometry-induced displacements to be simply additive, we would expect the superfluid transition to occur at around 1.65 K for $\bar{r} \approx 43$ Å. Even lower lambda temperatures are not unreasonable since the melting line of helium confined in bubbles can be displaced to higher pressures.[11,12] This expectation does not agree with our observed lowest peak temperatures of 1.8 K. The discrepancy may possibly result from the fact that bigger bubbles of the size distribution contribute more strongly to the heat-capacity peak and therefore increase T_p. Our lowest peak temperatures agree very well with those obtained by Thomson *et al.*[13] on pressurized helium in Vycor glass and by Gmelin and by Aslanian and Weil on helium bubbles in BeO.[2]

Our data show an additional bump or enhancement of the heat capacity in the range 2.5 K $< T <$ 5 K, whose size and position depends on the annealing temperature T_a. For small T_a this enhancement may result from the heat of melting of helium in bubbles at the low end of their size distribution ($r \lesssim 40$ Å). Such small bubbles do not exist for $T_a > 1100$ K. The enhancement of the heat capacity at $T \approx 2.8$ K after annealing at these higher T_a's may result from transformations occurring in submonolayer helium films,[14] existing on the inner surface of very large nonequilibrium bubbles (with $r \gtrsim 0.5$ μm). We have seen such bubbles, by scanning electron microscopy, decorating grain boundaries of our Cu sample.

The general increase of the heat capacity with increasing T_a is attributed to the continuing collection of helium from small into bigger bubbles, to the increase of the mass of *liquid* helium, to the decrease of its density, and to a "weakening" of the confinement with increasing $\bar{r}$. Subsequent measurements for samples with $\bar{r} > 60$ Å show heat-capacity data shifted almost parallel to each other. Subtracting the variable background of the data shown in Fig. 1, we see that the magnitude of the heat-capacity anomaly at T_p remained roughly constant for $\bar{r} > 60$ Å. This is in agreement with the observation that T_p did not increase in the same size range.

In this work we have introduced microscopic helium-filled bubbles in metals as a confining geometry to study size effects. This restricted geometry is highly uniform, allows simple variation of size, and can be visually investigated. We have applied this geometry to study the influence of size effects on the superfluid transition of liquid ^{4}He by low-temperature calorimetry. This transition was found to occur in bubbles with 43 Å $< r <$ 60 Å. These measurements were supplemented by TEM measurements of the variation of average radius, size distribution, and volume density of the helium-filled bubbles. The observed shifts of the lambda transition were explained by a combination of pressure and size effects in the bubbles, starting from the equation of state and our TEM results. The data also allowed us to interpret the solid-liquid transition in small bubbles as well as the formation of liquid-helium films on the surface of large bubbles. Future investigations at lower temperatures on ^{3}He to investigate the influence of this new confining geometry on a Fermi system are in progress.

We are indebted to Dr. P. Jung for the outgassing measurements on our specimens and to Dr. W. Kesternich for his support of this work.

---

[a]Present address.

[1]P. H. Keesom and G. Seidel, Phys. Rev. **111**, 422 (1958); O. P. Katyal, P. H. Keesom, and J. R. Cost, in *Proceedings of the International Conference on Radiation-Induced Voids in Metals,* edited by J. M. Corbett and L. L. Ianniello (Atomic Energy Commission, Washington, D.C., 1972).

[2]J. Aslanian and L. Weil, Cryogenics **3**, 36 (1963); E. Gmelin, J. Nucl. Mater. **38**, 150 (1971).

[3]H. J. von den Driesh and P. Jung, High Temp.–High Pressure **12**, 635 (1980); J. Laakmann, Kernforschungsanlage, Jülich, Report No. Jül-2007, 1985 (unpublished).

[4]J. C. Rife, S. E. Donnelly, A. A. Lucas, J.-M. Gilles, and J. J. Ritsko, Phys. Rev. Lett. **46**, 1220 (1981).

[5]W. Jäger, R. Manzke, H. Trinkaus, G. Crecelius, R. Zeller, J. Fink, and H. L. Bay, J. Nucl. Mater. **111&112**, 674 (1982).

[6]D. Schwahn, H. Ullmaier, D. Schelten, and W. Kesternich, Acta Metall. **31** 2003 (1983).

[7]H. Trinkaus, Radiat. Eff. **78**, 184 (1983).

[8]E. G. Syskakis, Kernforschungsanlage, Jülich, Report No. Jül-2012, 1985 (unpublished).

[9]R. S. Nelson, D. J. Mazey, and R. S. Barnes, Philos. Mag. **10**, 91 (1965).

[10]V. L. Ginzburg and A. A. Sobyanin, Usp. Fiz. Nauk **120**, 153 (1976) [Sov. Phys. Usp. **19**, 773 (1976)].

[11]E. N. Smith, D. F. Brewer, Cao Liezhao, and J. D. Reppy, Physica (Amsterdam) **107B+C**, 585 (1981).

[12]S. Balibar, D. O. Edwards, and C. Laroche, Phys. Rev. Lett. **42**, 782 (1979).

[13]A. L. Thomson, D. F. Brewer, T. Nagi, S. Haynes, and J. D. Reppy, Physica (Amsterdam) **107B+C**, 581 (1981).

[14]M. Bretz, J. G. Dash, D. C. Hickernell, E. O. Mc Lean, and O. E. Vilches, Phys. Rev. A **8**, 1589 (1973).

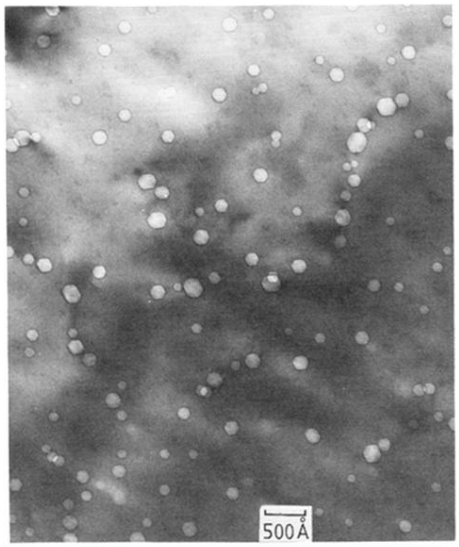

FIG. 2. A typical TEM picture of underfocused helium bubbles in Cu. The bubbles appear as light areas and are clearly faceted.